Cent. Eur. J. Chem. • 9(3) • 2011 • 415-421
DOI: 10.2478/s11532-011-0016-8

VERSITA

Central European Journal of **Chemistry**

$Na_{x-y}H_yTi_{2-x}Fe_xO_4 \bullet nH_2O$ nanosheets with lepidocrocite-like layered structure synthesized by hydrothermal treatment of ilmenite sand

Research Article

Paula M. Jardim[1*], Lidija Mancic[2], Bojan A. Marinkovic[1], Olivera Milosevic[2], Fernando Rizzo[1]

[1]*Departamento de Engenharia de Materiais, Pontifícia Universidade Católica do Rio de Janeiro, Gávea 22453-900, Rio de Janeiro, Brazil*

[2]*Institute of Technical Sciences of Serbia nA cademy of Sciences and Arts, Knez Mihailova 35/IV, 11000 Belgrade, Serbia*

Received 23 August 2010; Accepted 14 January 2011

Abstract: $Na_{x-y}H_yTi_{2-x}Fe_xO_4 \bullet nH_2O$ nanosheets with lepidocrocite-like layered structure were produced through alkaline hydrothermal treatment at very low temperatures (130°C) from ilmenite sand. The crystal structure, morphology and optical properties were investigated by X-Ray diffraction, transmission electron microscopy, selected area electron diffraction, energy dispersive spectroscopy and UV-Vis spectroscopy. The product shows leaf-like nanosheet morphology with thickness <30 nm and lengths <1 μm. Three lepidocrocite-like titanates (Imm2 space group) with similar a and c lattice parameters but different interlayer distances (b/2) were identified. This appears to be the first preparation of lepidocrocite-like layered nanosheets by a simple, energy efficient (low temperature) and low cost (starting from mineral sand) procedure.

Keywords: *Ilmenite • Hydrothermal synthesis • Lepidocrocite-like layered structure • X-ray diffraction • Transmission electron microscopy.*

1. Introduction

Lepidocrocite-like titanates have the general chemical formula $A_xTi_{2-y}M_yO_4$, and consist of two-dimensional layers of edge and corner-shared TiO_4 octahedra with interlayer alkali ions (A), usually with some interlayer water. Due to the substitution of lower-valence metal atoms or vacancies (M) in Ti sites, the layers have a negative charge compensated by the interlayer cations. The synthesis and characterization of several isomorphous lepidocrocite-like titanates have been reported with different combinations of M and A, where M can be Li, Mg, Zn, Cu, Co, Ni, Fe or a vacancy and A can be Cs, Rb, K, H, Na or Li [1-7]. Some examples are $H_xTi_{2-x/4}\square_xO_4 \bullet nH_2O$ (where $\square$ = vacancy) [1] , $K_xTi_{2-x/3}Li_{x/3}O_4$ [2] and $H_xTi_{2-x}Fe_xO_4 \bullet nH_2O$ [3].

This material can exfoliate layers into colloidal single sheets with subnanometer thickness by intercalation of bulky species such as tetrabutylammonium [8]. These nanosheets can be used as building blocks in the assembly of nanoarchitectures with controllable functionalities [9]. Titania nanosheets have attracted special attention because of their potential photocatalysis [10,11], photoconductivity [12] and photoluminescence [13-15]. Possible application in spin-electronic devices has motivated investigation of TiO_2 nanosheet-based ferromagnets ($Ti_{1-x}Co_xO_2$, $Ti_{1-x}Fe_xO_2$, $Ti_{1-x}Mn_xO_2$, $Ti_{0.8-x/4}Fe_{x/2}Co_{0.2-x/4}O_2$) [16-19].

All reported syntheses of lepidocrocite-like titanates used solid state reactions. Here we present a new method to produce $Na_{x-y}H_yTi_{2-x}Fe_xO_4 \bullet nH_2O$ lepidocrocite-like layered nanosheets: hydrothermal treatment of ilmenite sand. This synthesis is simple and energetically advantageous compared to solid state reactions as it requires very little heat (130°C). Moreover, the use of ilmenite sand, a very low cost precursor, makes it even more cost effective.

Compounds with a layered structure open a path for chemically controlled modifications through interlayer cation exchange, altering the physical properties. It has been reported [5,6] that the lower valence metal atoms M substituting Ti in the structure can also be removed

* *E-mail: paula@puc-rio.br*

by acid exchange. Thus, $Na_{x-y}H_yTi_{2-x}Fe_xO_4 \cdot nH_2O$ with a lepidocrocite-like layered structure might be modified to match its physical properties to an application.

In the present work the crystal structure, morphology and optical properties of $Na_{x-y}H_yTi_{2-x}Fe_xO_4 \cdot nH_2O$ nanosheets with lepidocrocite-like layered structure hydrothermally synthesized from ilmenite sand were investigated by X-Ray diffraction, transmission electron microscopy and UV-Vis spectroscopy.

2. Experimental Procedure

Untreated ilmenite sand from a Brazilian mine was used as a new low cost precursor (~$80 US ton^{-1}). It was ball milled for 90 min in a SPEX 8000-115 Mixer Mill with a 20:1 ball to ilmenite mass ratio, resulting in a mean particle size of 0.25 μm. In a typical synthesis 0.5 g of ball milled natural ilmenite sand was mixed with 25 mL of 10 M NaOH, transferred to a 30 mL Teflon-lined autoclave (83.3% filling factor) and held at 130°C for 70 h with continuous stirring. The resulting brown powder was dispersed in 200 mL of distilled water, mixed, and filtered. The powder was water washed (up to pH~7) and dried at 80°C for 5 h.

X-ray powder diffraction (XRPD) of precursor and product were performed on a RigakuXRD-6000powder diffractometer with CuKα radiation at 40 kV and 35 mA. LeBail analyses of XRPD patterns were carried out using Topas Academic software. Transmission electron microscopy (TEM) images, selected area electron diffraction (SAED) patterns and X-ray energy dispersive Spectrometry (EDS) were carried out in a JEOL-2010 microscope operating at 200 kV and in a Titan 80-300 microscope at 300 kV. TEM pecimens were prepared by ultrasonic dispersion of the powder in alcohol, then dropping onto a holey carbon film supported by a copper grid. Product compositions were determined by TEM/EDS. Scanning electron microscopy and EDS (SEM/EDS) were performed using a Zeiss DSM 960. Semi-quantitative X-Ray fluorescence (XRF) analysis (Software SemiQ PW2452) was performed in a Philips/Panalytical PW2400 with a Rh-based ceramic tube at 3 kVA. UV–Vis absorption spectra, analyzed in transmission mode, of the product suspension in water were obtained on an Agilent 8453 UV-vis spectrophotometer after 30 min of ultrasonication.

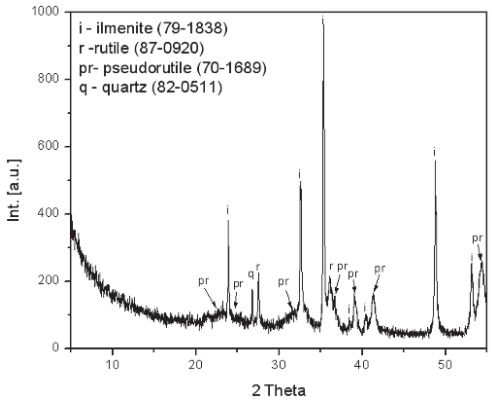

Figure 1. X-ray diffraction (XRD) of ilmenite sand precursor (numbers in parents correspond to powder diffraction file).

3. Results and Discussion

X-ray diffraction (XRD) of the ilmenite sand precursor, Fig. 1, shows that it consists of ilmenite as the principal crystal phase; however, pseudorutile, rutile and quartz are also present. X-Ray fluorescence (Table 1) and SEM/EDS (Fig. 2) also show that natural ilmenite sand is not homogeneous, having different impurity elements and phases. However, Fig. 2b (EDS) is consistent with Fig. 1, showing that ilmenite (gray phase in the backscatter image, Fig. 2a) is the principal phase in the sand.

LeBail refinement of the product XRD pattern (Fig. 3) clearly identified three Lepidocrocite-like titanates (space group: Imm2) with similar *a* and *c* lattice parameters but different interlayer distances (*b*/2), as well as a small amount of hematite nanoparticles (Table 2). The values obtained for *a* (~ 3.8 Å) and *c* (~ 3.0 Å) are similar to those reported by Reid *et al*. [4]: *a* = 3.805 Å and *c* = 2.972 Å, for $Cs_xTi_{2-x}Fe_xO_4$. EDS analysis (Fig. 4a) demonstrated the presence of Na, Fe, Ti and O. Because the samples were prepared in an aqueous environment and subsequently washed, partial ionic exchange of the interlayer cations (Na^+ by H^+) is plausible, suggesting that the product should be $Na_{x-y}H_yTi_{2-x}Fe_xO_4 \cdot nH_2O$. Therefore, the *a* and *c* lattice parameters (mostly dependent on the layer composition) should be similar to *a* and *c* for $Cs_xTi_{2-x}Fe_xO_4$. However, the interlayer distance (*b*/2) depends on the interlayer cation size and proportion (x) as well as the amount of interlayer water (n). Sasaki *et al*. [1] reported that interlayer distances in $Na_xTi_{2-x/4}\square_xO_4 \cdot nH_2O$ depend on the

Table 1. Semi-quantitative chemical analysis of natural Brasilian ilmenite sand.

SiO_2	1.74 wt%
TiO_2	55.7 wt%
Fe_2O_3	38.7 wt%
ZrO_2	0.20 wt%
Nb_2O_5	0.13 wt%
MnO	1.53 wt%
Al_2O_3	1.80 wt%

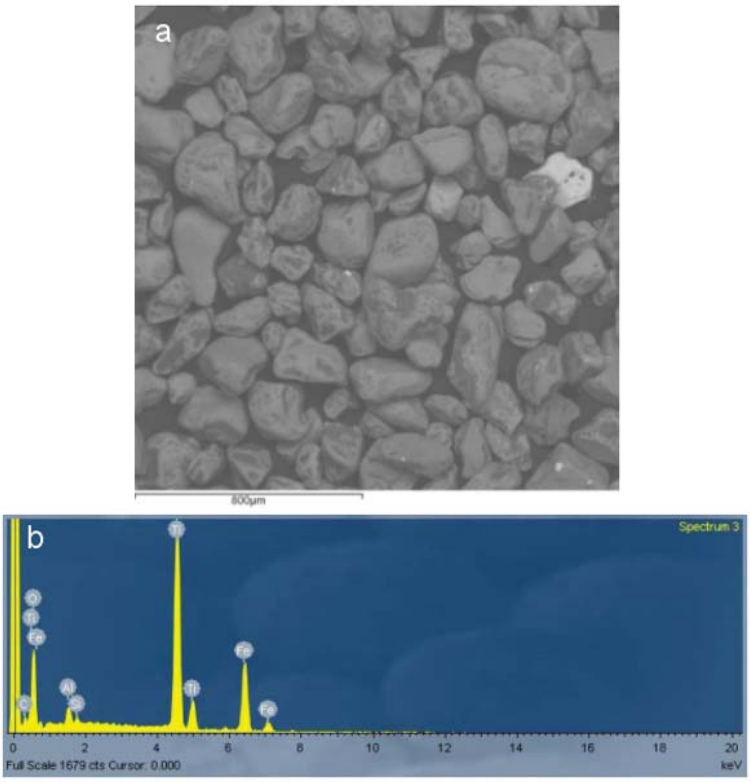

Figure 2. (a) SEM and (b) EDS of ilmenite sand.

Table 2. LeBail refinement results.

phase	Lepidocrocite-like titanate - 1	Lepidocrocite-like titanate - 2	Lepidocrocite-like titanate - 3	Hematite Fe_2O_3
Space group	Imm2	Imm2	Imm2	R-3cH
a (Å)	3.751	3.779	3.847	5.057
b (Å)	17.8	19.8	22.274	-
c (Å)	2.983	3.054	3.079	13.943
Interlayer distance (b/2)	8.9	9.9	11.137	-

r_exp = 7.036, r_exp_dash = 12.044, r_wp = 9.163, r_wp_dash = 15.686, r_p = 7.031, r_p_dash = 13.517, weighted_Durbin_Watson = 1.287, gof = 1.302

Na proportion (8.9 Å for x = 0.7 and 11.5 Å for x > 0.7). These values agree with two of the interlayer distances obtained for $Na_{x-y}H_yTi_{2-x}Fe_xO_4 \cdot nH_2O$ reported here (Table 2). The three interlayer distances obtained are due to inhomogeneous cation exchange (Na^+ for H^+) during washing resulting in particles with different proportions (x) of Na. Sasaki *et al*. [1] suggested that the phases with lower Na content and interlayer distance of ~9 Å are due to monolayers of cations and H_2O molecules in the galleries, while phases with higher Na content are likely to have a bilayer water/cation cluster, increasing the interlayer distance (*b*/2).

TEM analyses (Figs. 4-6) show leaf-like nanosheet morphology with thickness less than 30 nm and lengths below 1 µm. The TEM image in Fig. 4b shows both top views (beam perpendicular to the layers, parallel to [010]) and cross section views (beam parallel to the layers, perpendicular to [010]) of the nanosheets allowing thickness and length measurements. From Fig. 4c (HREM image of a nanosheet cross section) it was possible to measure the interlayer distance (*b*/2). The measured value, 7 Å, is well below the three values obtained from the XRD measurements. This can be explained by dehydration inside the TEM from the vacuum and heating by the beam. Sasaki *et al*. [1] reported interlayer contraction from 9.37 Å to 6.6 Å for $H_xTi_{2-x/4}\square_xO_4 \cdot nH_2O$ after dehydration, supporting our explanation. In agreement with the XRD results,hematite nanoparticles were also present, identified by the increased EDS Fe peak (Fig. 5a) and HREM lattice fringes spaced at 2.7 Å corresponding to hematite (104) planes (Fig. 5b).

As most of the nanosheets fell on the grid with [010] parallel to the beam the selected area diffractions patterns show a crystallographic texture, where the rings correspond to (*h*0*l*) or (*h*1*l*) planes. From the *a* and *c* parameters and the *b* value of ~14 Å, the interplanar distances between different crystallographic planes (*hkl*) were calculated to index the SADP (Fig. 6) acquired on the lepidocrocite-like product. The results agree with those reported by Sasaki *et al*. [20] for $H_xTi_{2-x/4}\square_xO_4 \cdot nH_2O$ exfoliated nanosheets.

It is well established that hydrothermal synthesis of layered titanates proceed by dissolution-precipitation [21]. The first step is ilmenite dissolution:

$$FeTiO_3 + NaOH \rightarrow Fe^{2+} + TiO_3^{2-} + Na^+ + OH^-$$

The oxidation state of Fe was assumed to be 2+, however, Fe^{3+} was present in the product as Fe_2O_3 (hematite) nanoparticles. There are two possible explanations. One is the oxidation of Fe^{2+} to Fe^{3+} during synthesis, while the other recognizes that natural ilmenite may also containing some Fe^{3+} accompanied by Ti^{3+} [22]. For partial substitution of Ti^{4+} by Fe^{3+} the formula will be $Na_xTi_{2-x}Fe_xO_4$ and if Ti^{4+} is partially substituted by Ti^{3+} and Fe^{3+} it will be $Na_x(Ti^{4+})_{2-x}(Fe^{3+}, Ti^{3+})_xO_4$. On the other hand, if Ti^{4+} is substituted by Fe^{2+} the formula will be $Na_xTi_{2-x/2}Fe_{x/2}O_4$. As we have no data on the Fe and Ti oxidation states we will assume the formula containing Fe^{3+} and Ti^{4+}, *i.e.*, $Na_xTi_{2-x}Fe_xO_4$. Therefore, the second step, crystallization of lepidocrocite-like nanosheets, can be represented by:

$$x\,Na^+ + x\,Fe^{3+} + (2-x)\,TiO_3^{2-} + z\,OH^- \rightarrow Na_xTi_{2-x}Fe_xO_4 + w\,H_2O$$

(where w = 2 + z-3x)

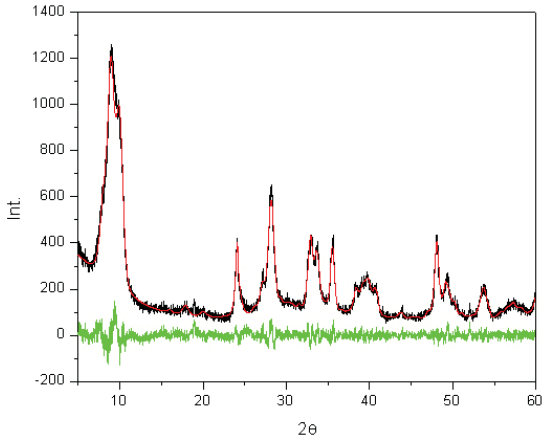

Figure 3. LeBail refinement of the hydrothermal product XRD.

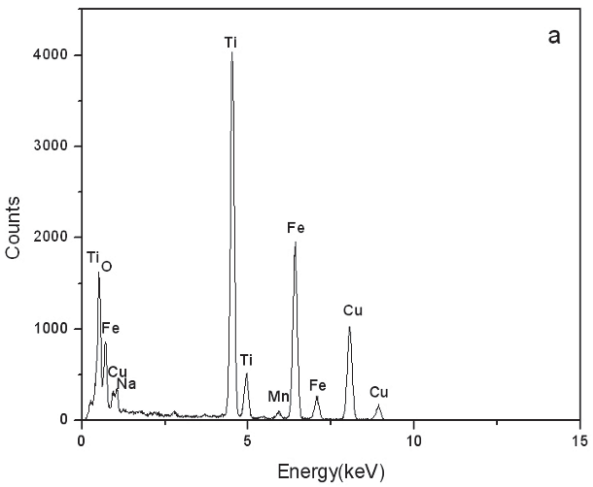

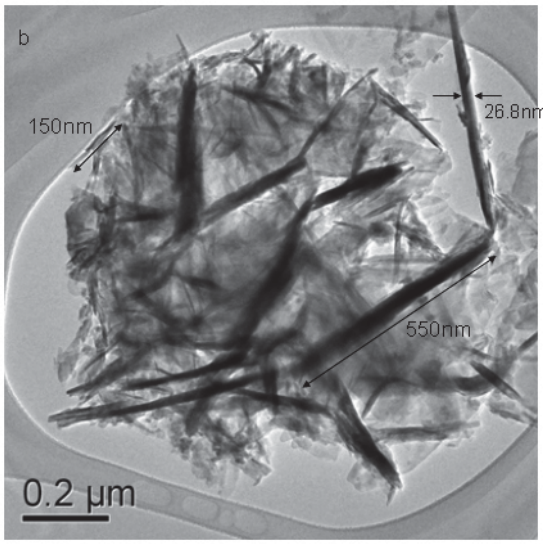

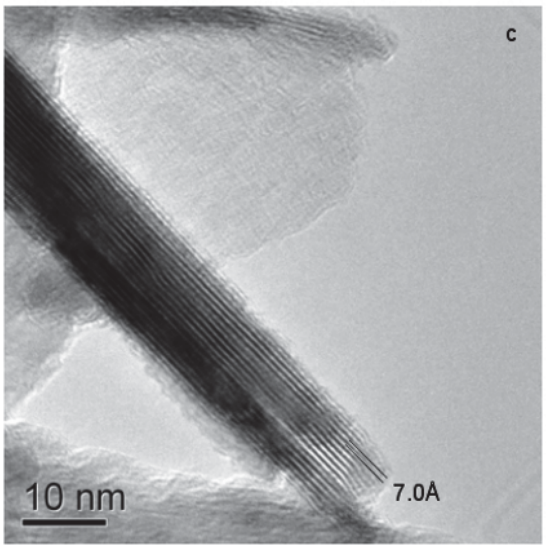

Figure 4. (a) EDS spectrum of the nanosheets exhibited in the TEM image (b), and (c) HREM image of a nanosheet cross section (beam perpendicular to [010]).

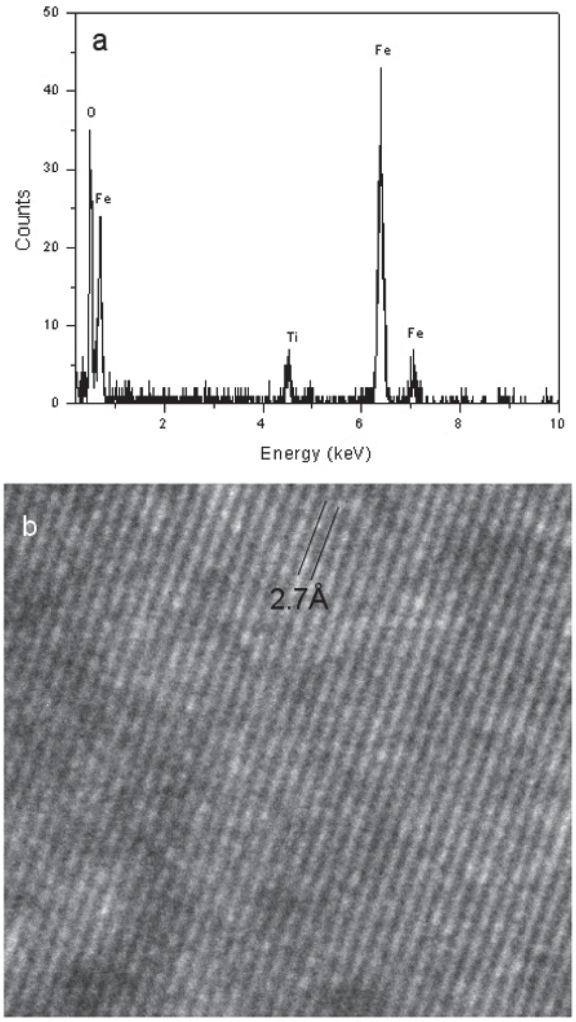

Figure 5. (a) EDS spectrum and (b) HREM image of hematite nanoparticles.

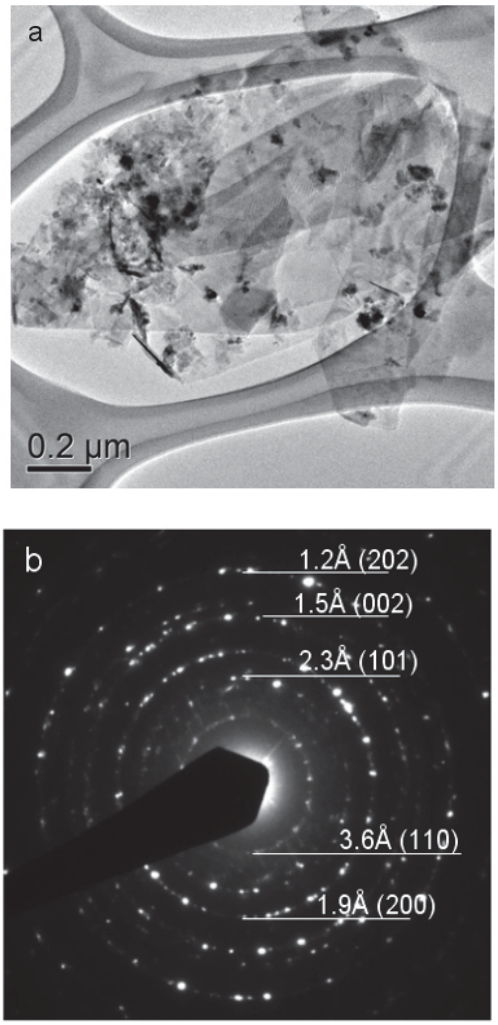

Figure 6. (a) TEM image of the $Na_{x-y}H_yTi_{2-x}Fe_xO_4 \cdot nH_2O$ nanosheets and (b) corresponding SADP.

The third step is the washing with H_2O, where interlayer cation exchange (Na^+ by H^+) takes place:

$$Na_xTi_{2-x}Fe_xO_4 + y\ H_2O \rightarrow Na_{x-y}H_yTi_{2-x}Fe_xO_4 + y\ NaOH$$

It is well known that H_2O molecules can be incorporated between TiO_2-based layers [1] resulting in a formula $Na_{x-y}H_yTi_{2-x}Fe_xO_4 \cdot nH_2O$. A feature observed in our previous work [23,24] on nanostructured layered titanates and also by Sasaki *et al*. [1] for $Na_xTi_{2-x/4}\square_xO_4 \cdot nH_2O$ is that the amount of interlayer water is proportional to the Na content. As this cation exchange was probably not homogeneous, resulting in three phases with different Na contents, different H_2O contents and interlayer distances resulted. To obtain a single phase (one interlayer distance) we plan longer washing times with aqueous HCl to completely displace Na^+ from the interlayer galleries by H^+.

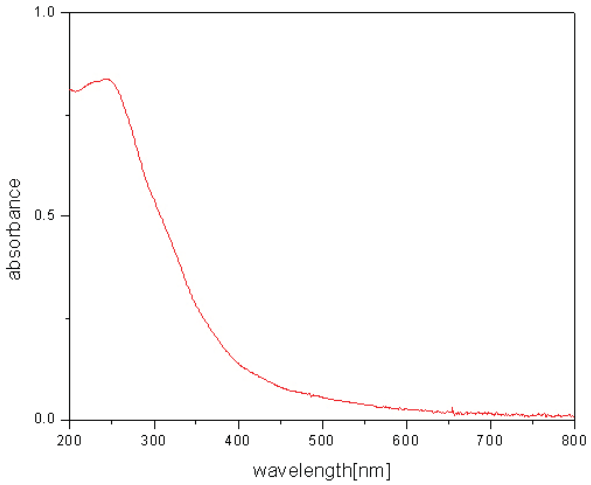

Figure 7. Optical absorption spectra of colloidal suspension of $Na_{x-y}H_yTi_{2-x}Fe_xO_4 \cdot nH_2O$ nanosheets.

Higher synthesis temperatures yield different products. Between 150°C and 170°C the product contains a mixture of $Na_{x-y}H_yTi_{2-x}Fe_xO_4 \cdot nH_2O$ leaf-like nanosheets, titanate nanobelts of the family $A_2Ti_xO_{2x+1} \cdot nH_2O$ (where A is the alkali metal cation often partially or fully exchanged for a proton) free of Fe and hematite nanoparticles. Further temperature increase yields $Na_xFe_xTi_{2-x}O_4$ with the $CaFe_2O_4$ crystal structure and arrow-like crystal morphology, as reported elsewhere [25].

To evaluate the optical properties and potential photocatalyst application an aqueous suspension of $Na_{x-y}H_yFe_xTi_{2-x}O_4 \cdot nH_2O$ nanosheets was analyzed by transmission UV-Vis absorption spectrophotometry (Fig. 7). The 5.11 eV peak is assigned the band gap energy. Sasaki *et al*. [26] analyzed $Ti_{1-x}\square_xO_2^{4x-}$ nanosheet crystallites by UV-Vis absorption and obtained a peak at 4.67 eV. They also estimated a band gap energy of 3.24 eV for the parent bulk layered compound $H_{0.7}Ti_{1.825}\square_{0.175}O_4 \cdot H_2O$ from a diffuse reflectance spectrum using the Kubelka-Munk method. Comparing these two values they attributed the blue shift to size quantization. The band gap (5.11 eV) obtained for $Na_yH_{x-y}Fe_xTi_{2-x}O_4 \cdot nH_2O$ nanosheets in the present work is close to the 4.67 eV obtained for $Ti_{1-x}\square_xO_2^{4x-}$ nanosheet crystallites by Sasaki *et al.* [26]. This indicates that lepidocrocite-like titanate nanosheets with thickness up to 30 nm (present work) show a significant band gap blue shift compared to bulk layered titanates or anatase (3.18 eV) and rutile (3.03 eV). Fig. 7 also shows a tail out to 600 nm (corresponding to ~2 eV) due to hematite, which has a 2.2 eV band gap [27].

4. Conclusions

$Na_{x-y}H_yTi_{2-x}Fe_xO_4 \cdot nH_2O$ nanosheets with lepidocrocite-like layered structure were synthesized from ilmenite sand for the first time by alkaline hydrothermal treatment at low temperatures (130°C). This process is energetically advantageous and cost effective compared to a solid state reaction, the most common process used to produce this type of material. TEM showed that the product has a leaf-like nanosheet morphology with thickness below 30 nm and lengths below 1 μm. Three Lepidocrocite-like titanates (Imm2 space group) with similar *a* and *c* lattice parameters and different interlayer distance (*b*/2), as well as a small amount of hematite were identified through LeBail refinement of the product XRDP. The three interlayer distances obtained were attributed to inhomogeneous cation exchange (Na^+ for H^+) during washing resulting in particles with different proportions (x) of Na. The band gap (5.11 eV) obtained for $Na_yH_{x-y}Fe_xTi_{2-x}O_4 \cdot nH_2O$ nanosheets in the present work is close to the 4.67 eV obtained for $Ti_{1-x}\square_xO_2^{4x-}$ nanosheet crystallites by Sasaki *et al*. [26].

Acknowledgement

L. Mancic and O. Milosevic gratefully acknowledge support from the Ministry of Science, Republic of Serbia (projects III 45020 and OI 172035).

L. Mancic expresses gratitude to the CNPq and FAPERJ, Brazilian Funding Agencies, for postdoctoral grants.

B. A. Marinkovic and P.M. Jardim are grateful to CNPq for financial support under the programs “Young Researchers in Nanotechnology” (62/2008), “MCT/CNPq 15/2007- Universal” and Research Productivity grants.

P.M. Jardim is grateful to S.M. Landi from INMETRO for assistance in operating the Titan 80-300.

References

[1] T. Sasaki, M. Watanabe, Y. Michiue, Y. Komatsu, F. Izumi, S. Takanouchi, Chem. Mater. 7, 1001 (1995)

[2] T. Sasaki, F. Kooli, M. Iida, Y. Machiue, Chem. Mater. 10, 4123 (1998)

[3] M. Hanada, T. Sasaki, Y. Ebina, M. Watanabe, Journal of Photochemistry and Photobiology A: Chemistry 148, 273 (2002)

[4] A.F. Reid, W.G. Mumme, A.D. Wadsley, Acta Cryst. B24, 1228 (1968)

[5] T. Gao, H. Fjellvag, P. Norby, Chem. Mater. 21, 3503 (2009)

[6] T. Gao, H. Fjellvag, P. Norby, J. Mater. Chem. 19, 787 (2009)

[7] T. Gao, P. Norby, H. Okamoto, H. Fjellvag, Inorg. Chem. 48, 9409 (2009)

[8] T. Sasaki, M. Watanabe, H. Hashizume, H. Yamada, Nakazawa, J. Am. Chem. Soc. 118, 8329 (1996)

[9] M. Osada, T. Sasaki, J. Mater. Chem. 19, 2503 (2009)

[10] N.Sakai, K. Fukuda, T. Shibata, Y. Ebina, K. Takada, T. Sasaki, J. Phys. Chem. B 110, 6198 (2006)
[11] T. Shibata, N. Sakai, K. Fukuda, Y. Ebina, K. Takada, T. Sasaki, Phys. Chem. Chem. Phys. 9, 2413 (2007)
[12] N. Sakai, Y. Ebina, K. Takada, T. Sasaki, J. Am. Chem. Soc. 126, 5851 (2004)
[13] T.C. Ozawa, K. Fukuda, K. Akatsuka, Y. Ebina, T. Sasaki, Chem. Mater. 19, 6575 (2007)
[14] T.C. Ozawa, K. Fukuda, K. Akatsuka, Y. Ebina, T. Sasaki, K. Kurashima, K. Kosuda, J. Phys. Chem. C 112, 1312 (2008)
[15] S. Ida, C. Ogata, U. Unal, K. Izawa, T. Inoue, O. Altuntasoglu, Y. Matsumoto, J. Am. Chem. Soc. 42, 4092 (2003)
[16] M. Osada, Y. Ebina, K. Takada, T. Sasaki, Adv. Mater. 18, 295 (2006)
[17] M. Osada, Y. Ebina, K. Fukuda, K. Ono, K. Takada, K. Yamaura, E. Takayama-Muromachi, T. Sasaki, Phys. Rev. B 73, 153301 (2006)
[18] M. Osada, M. Itose, Y. Ebina, K. Ono, S. Ueda, K. Kobayashi, T. Sasaki, Appl. Phys. Lett. 92, 253110 (2008)
[19] Z. Liu, R. Ma, M. Osada, N. Iyi, Y. Ebina, K. Takada, T. Sasaki, J. Am. Chem. Soc.128, 4872 (2006)
[20] T. Sasaki, Y. Ebina, Y. Kitami, M. Watanabe, J. Phys. Chem. B 105, 6116 (2001)
[21] D.V. Bavykin, V.N. Parmon, A.A. Lapkina, F.C. Walshc, J. Mater. Chem. 14, 3370 (2004)
[22] X. Wu, G. Steinle-Neumann, O. Narygina, I. Kantor, C. McCammon, S. Pascarelli, G. Aquilanti, V. Prakapenka, L. Dubrovinsky, Phys. Rev. B 79, 094106 (2009)
[23] E. Morgado Jr., M.A.S. de Abreu, O.R.C. Pravia, B.A. Marinkovic, P.M. Jardim, F.C. Rizzo, A.S. Araújo, Solid State Sciences 8, 888 (2006)
[24] E. Morgado, Jr., M.A.S. de Abreu, G.T. Moure, B.A. Marinkovic, P.M. Jardim, A.S. Araujo, Chem. Mater. 19, 665 (2007)
[25] B.A. Marinkovic, L. Mancic, P.M. Jardim, O. Milosevic, F. Rizzo, Solid State Commun. 145, 346 (2008)
[26] T. Sasaki, M. Waranabe, J. Phys. Chem. B, 101, 10159 (1997)
[27] B. Gilbert, C. Frandsen, E.R. Maxey, D.M. Sherman, Phys. Rev. 79, 035108 (2009)